Geologie en Mijnbouw **75:** 275–282, 1996.

Strontium-isotope stratigraphy of the type Maastrichtian and the Cretaceous/Tertiary boundary in the Maastricht area (SE Netherlands)

H.B. Vonhof & J. Smit
Institute of Earth Sciences, Vrije Universiteit, De Boelelaan 1085, 1081 HV Amsterdam, the Netherlands

Received 29 September 1995; accepted in revised form 9 May 1996

Key words: diagenesis, K/T boundary, Geulhemmerberg

Abstract

The comparison of a detailed $^{87}Sr/^{86}Sr$ profile through the Maastrichtian of the ENCI, Curfs and Geulhemmerberg quarries in the Maastrichtian type area with a Late Maastrichtian to Early Danian seawater $^{87}Sr/^{86}Sr$ curve of the Bidart (France) and El Kef (Tunisia) sections provides a useful chronostratigraphy for these quarries. The best fit yields an accumulation rate of ~ 10 cm/ka for the upper 30 m of the Maastrichtian in the composite Curfs and ENCI section. Apparently, despite diagenetic alteration, the fossils from the Curfs and ENCI quarries partly retained their original seawater $^{87}Sr/^{86}Sr$ values.

$^{87}Sr/^{86}Sr$ analyses of well-preserved heterohelicids in the Geulhemmerberg E-clay support the suggested Early Danian age of this clay. They also support the suggestion that the planktic foraminifer *Heterohelix globulosa* survived the Cretaceous/Tertiary boundary event(s) for some 5 to 50 ka.

Introduction

Marine carbonate and phosphate fossils can be dated by fitting the $^{87}Sr/^{86}Sr$ ratio of the fossil into a well-dated seawater $^{87}Sr/^{86}Sr$ reference curve. In analogy with the Sr-isotope systematics in modern seawater, two main assumptions underlie the method, viz. 1) the $^{87}Sr/^{86}Sr$ ratio of marine carbonate or phosphate equals that of the coeval seawater, and 2) at any given point in time, the oceans are well mixed with respect to Sr, resulting in a homogeneous $^{87}Sr/^{86}Sr$ ratio.

The seawater $^{87}Sr/^{86}Sr$ reference curves have been established and are continuously updated for most of the Phanerozoic (Beets 1991; Burke et al. 1982; Hess et al. 1986; Hodell et al. 1991; Peterman et al. 1970). Uncertainties of these reference curves increase with age, which is mostly due to the deteriorating preservation state and availability of fossils suitable for analyses, and to the decreasing resolution of time calibration with age.

The time interval around the Cretaceous/Tertiary (K/T) boundary has been studied in more detail than other intervals, in order to check on the occurrence and magnitude of a sharp radiogenic ^{87}Sr-spike exactly at the boundary first reported by Hess et al. in 1986 (Jones et al. 1987; Martin and Macdougall 1991; Meisel et al. 1995; Nelson et al. 1991; Swinburne et al. submitted). Some workers still doubt if this spike really existed in seawater at the time (Jones et al. 1987; McArthur 1994; Nelson et al. 1991; Swinburne et al. submitted). Others do find the spike but disagree on its magnitude (Hess et al. 1986; Javoy and Courtillot 1989; Martin and Macdougall 1991; Meisel et al. 1995; Vonhof and Smit in prep.). Reported shifts in the $^{87}Sr/^{86}Sr$ ratio range from 0.000028 (Martin and Macdougall 1991) to 0.0002 (Javoy and Courtillot 1989).

Diagenetic processes can alter the $^{87}Sr/^{86}Sr$ ratio of a fossil, resulting in an erroneous Sr-isotopic age. For that reason, when using diagenetically altered samples, one has to establish the Sr-isotopic record for a time interval in several stratigraphic sections, each with possibly different diagenetic histories. We used this method to construct a detailed reference section for the Late Maastrichtian by matching the $^{87}Sr/^{86}Sr$ records of El Kef (Tunisia) and Bidart (France). The resulting $^{87}Sr/^{86}Sr$ reference curve shows a Late Maastrichtian maximum at 300–400 ka before the K/T boundary and

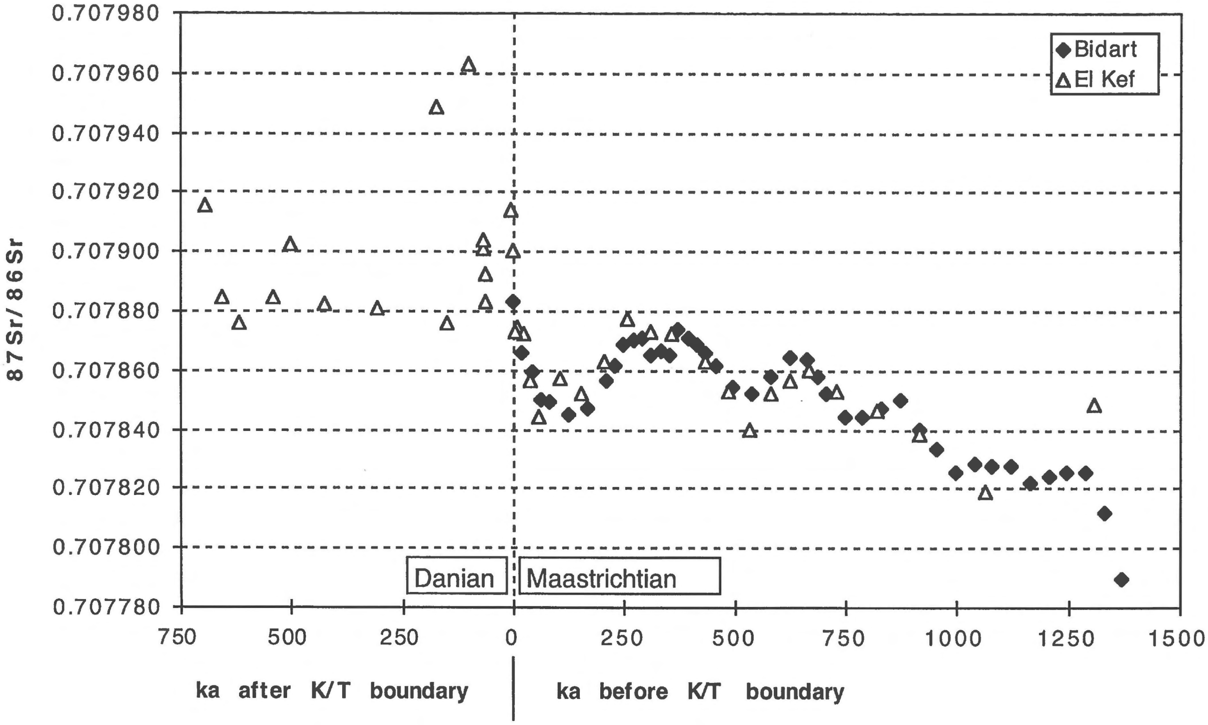

Figure 1. The combined $^{87}Sr/^{86}Sr$ records of the Bidart and El Kef sections taken from Vonhof and Smit (in preparation), used as the seawater $^{87}Sr/^{86}Sr$ reference curve for the Cretaceous–Tertiary interval in this study. The Maastrichtian time frame is based on Milankovitch precession cycles in the Bidart section. The Danian time frame is based on biostratigraphy.

a sharp $\pm$ 0.0001 radiogenic shift at the boundary itself (Figure 1; Vonhof and Smit, in prep.).

The goal of this paper is to compare this reference curve with a composite record, hereafter referred to as the CEG section, from samples taken in the Curfs, ENCI and Geulhemmerberg quarries in southern Limburg (the Netherlands). In the Geulhemmerberg section, only a single stratigraphic level was sampled at the site described by Brinkhuis and Smit (this issue). This level is the so-called E-clay which is correlated with a clay-flake level in the Curfs quarry (Roep and Smit, this issue; see Figure 2).

Methods

Foraminifera and fragments of other fossils were hand-picked and cleaned ultrasonically in ethanol. Light and scanning-electron microscopic (SEM) examination, cathodo-luminescence images, and X-ray-fluorescence-derived Sr abundances served to evaluate diagenetic alteration.

Per sample, 0.5 to 3.0 mg of $CaCO_3$ was dissolved in 1.0 to 1.5 N. hydrochloric acid or in 5 N. acetic acid, and centrifuged for 5 min at 4000 rpm. The supernatant was removed within 15 min from the start of the reaction to prevent leaching of Sr from the remnant non-carbonate fraction. Laboratory tests showed reproducible $^{87}Sr/^{86}Sr$ results for aliquots dissolved in 5 N. acetic acid and 1.5 N. hydrochloric acid (Beets, 1991). Strontium separation took place by ion exchange using 0.15 ml Elchrom SrSPEC® resin per sample. The resulting Sr was analysed on a single rhenium filament in a solid-source Finnigan 261 mass spectrometer. The standard analyses program produces 8 blocks of 10 runs each (n = 80). Routine analyses yield a 2 standard error (2 s.e.) value of 0.000010 or less. Analyses were rejected at 2 s.e. values of 0.000015 or more. Over the two years in which the analyses were carried out, the NBS 987 standard laboratory average was 0.710275, normalized for $^{86}Sr/^{88}Sr = 0.1194$.

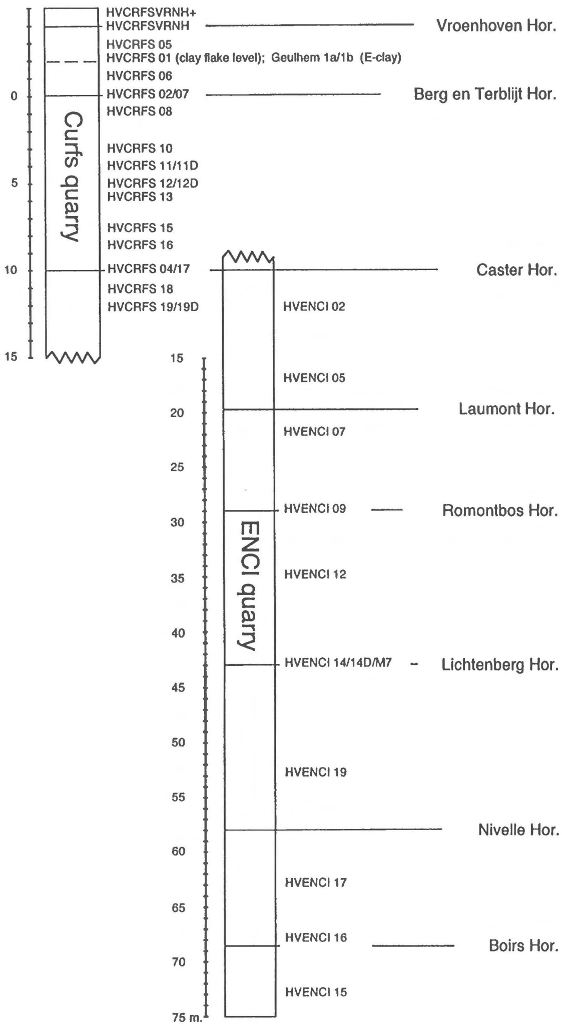

Figure 2. A schematic stratigraphic column of the sampled sections in the Curfs (left) and ENCI (right) quarries. Sample locations and regional 'horizons' are indicated. The E-clay samples from the Geulhemmerberg section (Geulhem 1a, b) are placed at the corresponding stratigraphic level in the Curfs column. For a detailed Geulhemmerberg column see Brinkhuis and Smit (this issue).

Results

Table 1 lists all data, and Figure 3a shows the $^{87}Sr/^{86}Sr$ data of the composite CEG section at 10 cm/ka sedimentation rate cross-plotted with the El Kef-Bidart reference $^{87}Sr/^{86}Sr$ curve. The CEG data generally plots too high to fit the reference curve, which suggests the presence of a radiogenic diagenetic overprint. A $^{87}Sr/^{86}Sr$ versus 1/Sr ppm plot for the Curfs quarry (Figure 4) shows that $^{87}Sr/^{86}Sr$ ratios increase with decreasing Sr abundances. Since diagenesis generally decreases the Sr abundance, this also indicates a relatively radiogenic overprint. Euhedral diagenetic calcite crystals are visible on SEM photographs (Figure 5) and diagenesis also shows on cathodo-luminescence images (Kenter et al., submitted).

Discussion

Diagenesis

Carstic features, formed at the top of the carbonate succession of the Curfs quarry, sometimes reach down into Maastrichtian strata. Carst-dissolution of relatively radiogenic Sr in the Paleocene Houthem Formation, and the subsequent recrystallisation of the dissolved carbonate in the underlying Maastrichtian limestones may partly explain the observed radiogenic $^{87}Sr/^{86}Sr$ shift in the Maastrichtian record. Likewise, more recent meteoric diagenesis in the succession can be expected to have contributed more radiogenic $^{87}Sr/^{86}Sr$ values as well. This, since overlying strata, potentially supplying the diagenetic Sr, typically have higher $^{87}Sr/^{86}Sr$ values.

Maastrichtian Sr-isotope stratigraphy for the CEG section

Despite the alteration, the $^{87}Sr/^{86}Sr$ data of the CEG section still shows the general pattern of the El Kef-Bidart reference curve, especially when an eye-ball fit curve is drawn through the lower, presumably least altered, CEG $^{87}Sr/^{86}Sr$ ratios (Figure 3b). The Late Maastrichtian $^{87}Sr/^{86}Sr$ maximum, at 300–400 ka before the K/T boundary in the El Kef-Bidart reference curve, is approximately located at the Romontbos Horizon in the CEG section. Assuming a constant sedimentation rate, our best fit for this CEG eye-ball fit curve with the El Kef-Bidart reference curve is at a 10 cm/ka sedimentation rate for the CEG section (Figure 3a), with an estimated uncertainty of $\pm$ 2 cm/ka. This is in agreement with biostratigraphic estimates of 5–10 cm/ka for the section above the Lichtenberg Horizon (J. Jagt, personal communication), and with the 8 cm/ka estimated from the analyses of Milankovitch cycles above the Laumont Horizon in the ENCI quarry (Zijlstra 1994). The $^{87}Sr/^{86}Sr$ stratigraphic control on the lower part of the section, below the Romontbos Horizon, is poor. A change in the sediment composition at the Lichtenberg Horizon suggests lower sedi-

Table 1. Strontium-isotopic and abundance data for the samples from the CEG section. See Figure 2 for sample positions. Stratigraphic level in meters below K/T (Berg en Terblijt Horizon); underlined values are above this horizon. Carbon and oxygen-isotopic data for Geulhemmerberg E-clay foraminifera are also shown.

Sample	Strat. level	$^{87}Sr/^{86}Sr$	2 st. error	Sr ppm	Material
HVCRFSVRNH+	4.20	0.707932	0.000009	482	bryozoan fragm.
HVCRFSVRNH	4.00	0.707886	0.000008	477	bulk
HVCRFS05	2.50	0.707892	0.000010	482	shell fragment
HVCRFS01	2.00	0.707927	0.000014	507	*Orbitoides*
HVCRFS06	1.00	0.707919	0.000012		shell fragment
HVCRFS02	0.00	0.707904	0.000013	537	*Orbitoides*
HVCRFS07	0.00	0.707875	0.000010	541	*Orbitoides*
HVCRFS08	1.00	0.707895	0.000010	503	shell fragment
HVCRFS10	3.00	0.707866	0.000010	509	bryozoan fragm.
HVCRFS11	4.00	0.707922	0.000012	470	*Orbitoides*
HVCRFS11 D.	4.00	0.707892	0.000009	490	bryozoan fragm.
HVCRFS12	5.00	0.707893	0.000008	464	*Orbitoides*
HVCRFS12 D.	5.00	0.707884	0.000008	506	bryozoan fragm.
HVCRFS13	5.70	0.707858	0.000010	572	bryozoan fragm.
HVCRFS15	7.70	0.707868	0.000008	540	bryozoan fragm.
HVCRFS16	8.70	0.707854	0.000010		shell fragment
HVCRFS04	10.00	0.707883	0.000014		oyster
HVCRFS17	10.00	0.707855	0.000010	548	oyster
HVCRFS18	11.00	0.707857	0.000010	787	shell fragment
HVCRFS19	12.00	0.707899	0.000010	611	oyster
HVCRFS19 D.	12.00	0.707877	0.000009	617	bryozoan fragm.
HVENCI02	12.00	0.707862	0.000009	419	shell fragment
HVENCI05	17.00	0.707845	0.000008		shell fragment
HVENCI07	22.00	0.707881	0.000007		shell fragment
HVENCI09	29.00	0.707895	0.000012		bulk
HVENCI12	35.00	0.707892	0.000008		bulk
HVENCI14	43.00	0.707950	0.000008		shell fragment
HVENCI14 D.	43.00	0.707905	0.000010		bryozoan fragm.
M7	43.00	0.707879	0.000007		shell fragment
HVENCI19	53.00	0.707902	0.000008		shell fragment
HVENCI17	63.00	0.707862	0.000008		ostracods
HVENCI16	68.00	0.707872	0.000010		ostracods
HVENCI15	73.00	0.707894	0.000010		ostracods
Geulhem 1a	2.00	0.707932	0.000013	1340	*H. globulosa*
Geulhem 1b	2.00	0.707913	0.000010		*H. globulosa*
NBS 987		0.710275			lab Sr standard

Sample	Strat, level	$\delta^{13}C$‰ vs PDB	$\delta^{18}O$‰ vs PDB		Material
Geulhem 1a	2.00	1.31	- 1.80		*H. globulosa*
Geulhem 1b	2.00	1.69	- 0.81		bulk benth. forams

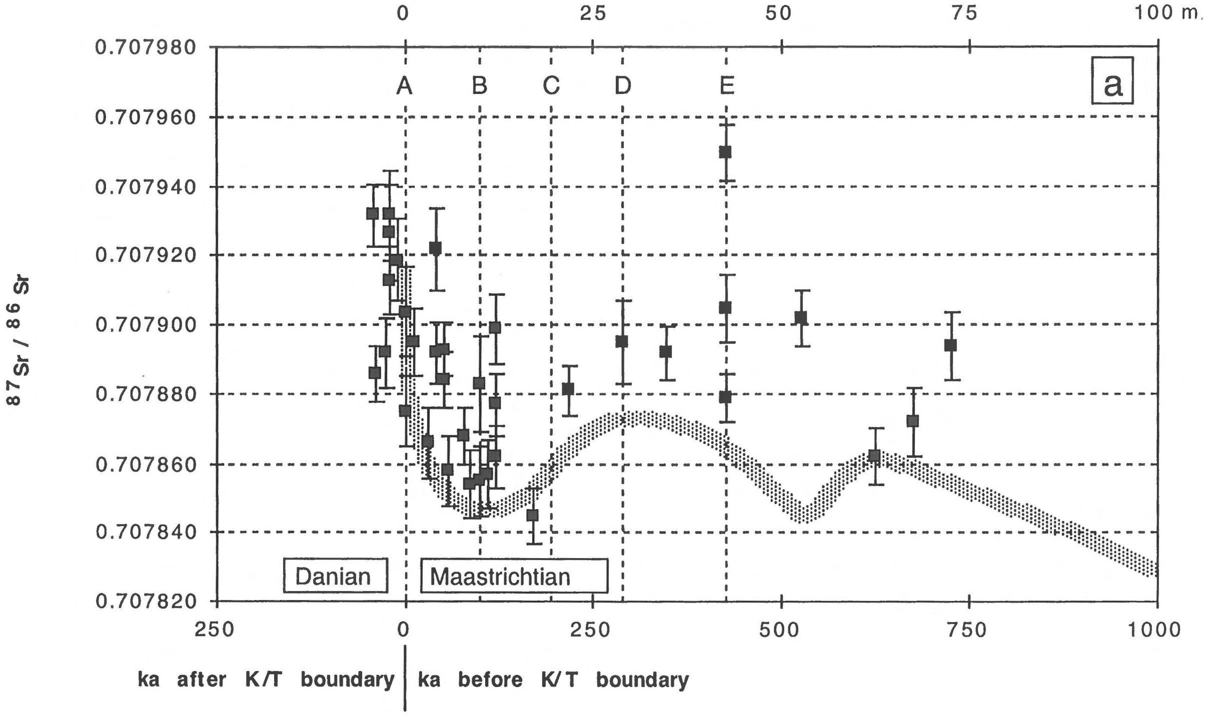

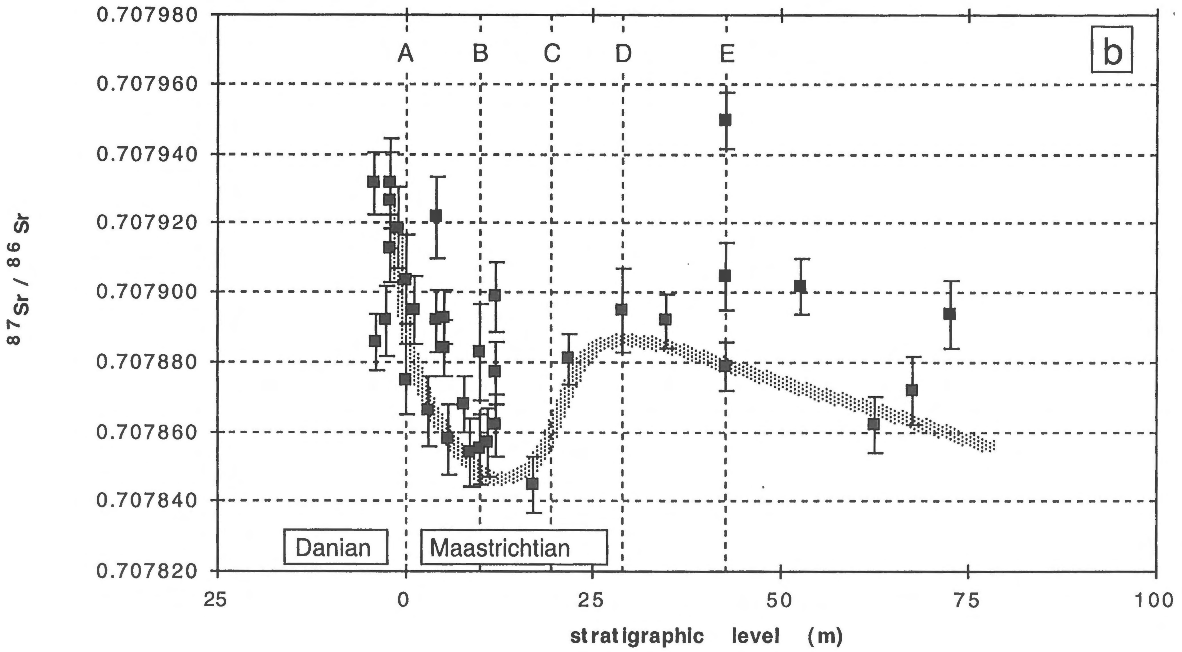

Figure 3. Plots of the $^{87}Sr/^{86}Sr$ data (Table 1) of the Curfs-ENCI-Geulhemmerberg (CEG) section. A = Berg en Terblijt Horizon, B = Caster Horizon, C = Laumont Horizon, D = Romontbos Horizon, E = Lichtenberg Horizon. Error bars are 2 s.e. values. a) CEG data cross-plotted with the El Kef-Bidart reference curve (shaded, cf. Figure 1) at 10 cm/ka sedimentation rate for the CEG section. The time scale at the bottom of the graph is derived from the reference curve, the meter scale at the top corresponds to the stratigraphic position of the CEG data (0 at K/T boundary for both scales). b) CEG data superimposed on an eye-ball fit curve through the lower values (shaded, see text). The meter scale corresponds to the stratigraphic position of the CEG data (0 at the K/T boundary).

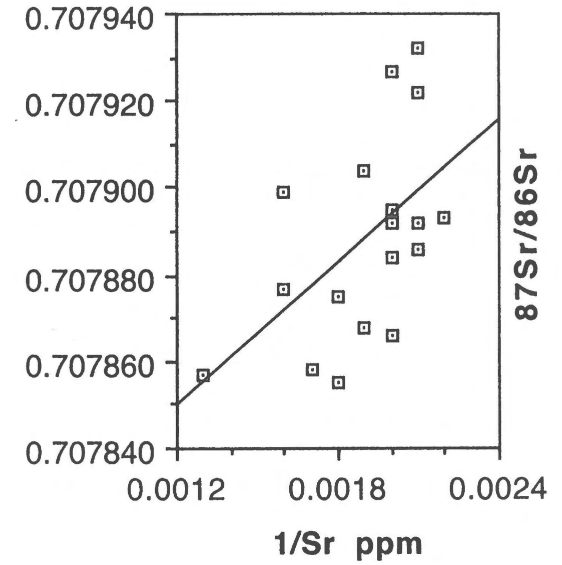

Figure 4. $^{87}Sr/^{86}Sr$ values versus the inverse of the Sr abundance (1/ppm) for the Curfs quarry (Table 1). Binary mixing between an original seawater end member and a diagenetic end member should result in a linear correlation. Despite the scatter, there appears to be a significant trend showing increasing $^{87}Sr/^{86}Sr$ values with decreasing Sr abundance, indicating a relatively radiogenic diagenetic end member. The solid line represents the linear regression calculated for the data.

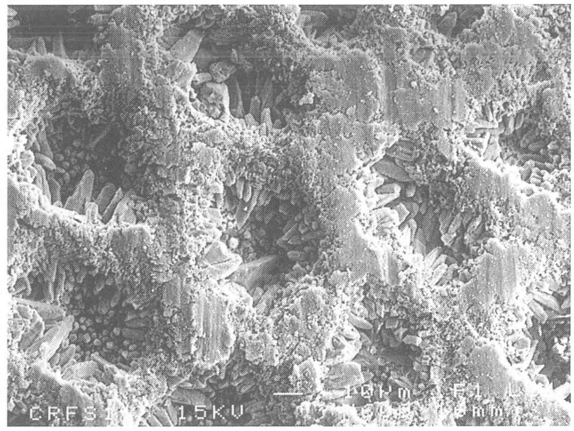

Figure 5. An illustration of the preservation state of Maastrichtian carbonate fossils from the Curfs and ENCI quarries. The photograph shows diagenetic calcite grown into the chambers of an *Orbitoides* sp.

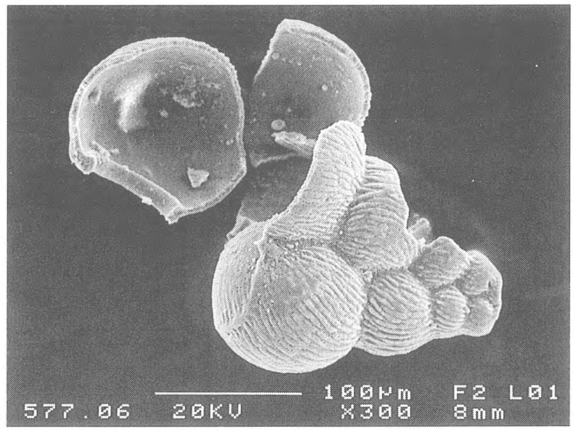

Figure 6. A specimen of *Heterohelix globulosa* taken from the Geulhemmerberg E-clay. Virtually all planktic foraminifera from this clay are air-filled, and appear unaltered. We have crushed the top chamber of this specimen to illustrate the absence of sediment or diagenetic calcite in the chambers.

mentation rates for the finer grained sediments below this horizon. Furthermore, the large scatter in the three $^{87}Sr/^{86}Sr$ values for the horizon itself indicates that, also for the lower part of the CEG section, the recorded $^{87}Sr/^{86}Sr$ values are probably offset by diagenesis in the same way as in the top of the section. Therefore, the Sr-isotopic ages for the CEG section below the Romontbos Horizon in Figure 3a should be seen as minimum ages, because we can only guess how much even the lowest $^{87}Sr/^{86}Sr$ values are diagenetically offset. If we assume that the average diagenetic offset below the Romontbos Horizon is comparable to the offset in the top part of the CEG section, then we would estimate a minimum $^{87}Sr/^{86}Sr$ value of 0.707840, resulting in a maximum age of 1 Ma before the K/T boundary, for the base of the ENCI quarry. Going towards the Campanian/Maastrichtian boundary, $^{87}Sr/^{86}Sr$ ratios for the reference curve will only decrease more, making older ages for the base of the ENCI quarry less probable. Additional $^{87}Sr/^{86}Sr$ analyses, combined with a more detailed geochemial examination of the preservation state of the samples, can add a more solid background to these estimates.

Sr-isotope stratigraphy of the Geulhemmerberg quarry

The clay layers in the underground Geulhemmerberg quarry, in particular the E-clay, are biostratigraphically of Early Danian age (Brinkhuis and Schiøler; Willems; Smit and Zachariasse; Romein et al., this issue). In the absence of an Ir anomaly, the lowermost Danian, containing the impact ejecta, is believed to be missing (Smit and Rocchia, this issue). The ~ 10 cm-thick, very fresh and uncompacted E-clay appears not bioturbated, apart from a few single burrows. It contains a low-diversity planktic foraminiferal fauna, dominated by air-filled specimens of *Heterohelix globulosa* (Ehrenberg) (Figure 6).

Due to the sealing capacity of the clay, the heterohelicids are well preserved. SEM study did not reveal any sign of alteration, apart from some minor dissolution features. $\delta^{18}O$ values vs PDB of minus 1.80 ± 0.1‰ and a 1340 ppm Sr abundance for these foraminifera do not indicate alteration either. The good preservation of organic matter in the clay (Yamamoto et al., this issue), is yet another indication of the clay's sealing capacity.

$^{87}Sr/^{86}Sr$ ratios of the heterohelicids are incompatible with the Late Maastrichtian seawater $^{87}Sr/^{86}Sr$ ratios of the El Kef-Bidart reference curve, but match the higher ratios of the earliest Danian. Therefore, we regard these $^{87}Sr/^{86}Sr$ values as supporting evidence for the Early Danian age of the E-clay. In the absence of Ir, this implies that *H. globulosa* survived the K/T boundary event for at least the duration of deposition of the Ir-bearing K/T boundary clay known from many other sections, which is estimated at 5–50 ka (Keller and Barrera 1990; Keller et al. 1993; Smith and Romein 1985).

Conclusions

Despite a radiogenic diagenetic overprint, the pattern of the Late Maastrichtian seawater Sr-isotopic ratios can still be recognised in the top part of the composite Curfs and ENCI section. The resulting average sedimentation rate from the Romontbos Horizon up to the Berg en Terblijt Horizon is ± 10 cm/ka.

Specimens of the planktic foraminifer *Heterohelix globulosa* in the Geulhemmerberg E-clay appear very well preserved. Their $^{87}Sr/^{86}Sr$ ratio matches that of early Danian seawater. In the absence of Ir, we conclude that they have survived the K/T boundary for at least some 5–50 ka, the duration of deposition of the Ir-bearing boundary clay found in other K/T boundary sections (El Kef, Bidart).

This is contribution 960805 of the Netherlands Research School of Sedimentary Geology (NSG).

References

Beets, C.J. 1991 The Late Neogene $^{87}Sr/^{86}Sr$ isotopic record in the western Arabian Sea, Site 722. In: W.L. Prell & N. Niitsuma (eds): Proc. Ocean Drilling Program, Scientific Results 117: 459–463

Brinkhuis, H. & P. Schiøler (this issue) Palynology of the Geulhemmerberg Cretaceous/Tertiary boundary section (Limburg, SE Netherlands)

Brinkhuis, H. & J. Smit (this issue) The Geulhemmerberg Cretaceous/Tertiary boundary section (Maastrichtian type area, SE Netherlands); an introduction

Burke, W.H., R.E. Denison, E.A. Hetherington, R.B. Koepnick, H.F. Nelson & J.B. Otto 1982 Variation of seawater $^{87}Sr/^{86}Sr$ throughout Phanerozoic time – Geology 10: 516–519

Hess, J., M.L. Bender & J.G. Schilling 1986 Evolution of the Ratio of Strontium-87 to Strontium-86 in seawater from Cretaceous to Present – Science 231: 979–984

Hodell, D.A., P.A. Mueller & J.R. Garrido 1991 Variations in the strontium isotopic composition of seawater during the Neogene – Geology 19: 24–27

Jones, D.A., P.A. Mueller, J.R. Bryan, J.P. Dobson, J.E.T. Channel, J.C. Zachos & M.A. Arthur 1987 Biotic, geochemical, and paleomagnetic changes across the Cretaceous/Tertiary boundary at Braggs, Alabama – Geology: 311–315

Keller, G. & E. Barrera 1990 The Cretaceous-Tertiary boundary impact hypothesis and the Paleontological record. In: V.L. Sharpton & P.D. Ward (eds): Global Catastrophes in Earth History; An Interdisciplinary Conference on Impacts, Volcanism, and Mass Mortality – Geol. Soc. Am. Spec. Paper 247: 563–575

Keller, G., E. Barrera, B. Schmitz & E. Mattson 1993 Gradual mass extinction, species survivorship, and long-term environmental changes across the Cretaceous Tertiary boundary in high latitudes – Geol. Soc. Am. Bull. 105: 979–997

Kenter, J.A.M., B.W. Fouke, Y.Y. Podlachikov & M. Reinders (submitted) Effects of differential compaction on the accoustic properties and permeability of Upper Cretaceous limestones (SE Netherlands) – J. Sedimentary Research

Martin, E.E. & J.D. Macdougall 1991 Seawater Sr isotopes at the Cretaceous/Tertiary boundary – Earth Planet. Sci. Lett. 104: 166–180

McArthur, J.M. 1994 Recent trends in strontium isotope stratigraphy – Terra Nova 6: 331–358

Meisel, T., U. Krähenbühl & M.A. Nazarov 1995 Combined osmium and strontium isotopic study of the Cretaceous-Tertiary boundary at Sumbar, Turkmenistan: A test for an impact vs. a volcanic hypothesis – Geology 23: 313–316

Nelson, B.K., G.K. MacLeod & P.D. Ward 1991 Rapid change in strontium isotopic composition of sea water before the Cretaceous/Tertiary boundary – Nature 351: 644–646

Peterman, Z.E., C.E. Hedge & H.A. Tourtelot 1970 Isotopic composition of strontium in sea water throughout Phanerozoic time – Geochim. Cosmochim. Acta 34: 105–120

Roep, Th.B. & J. Smit (this issue) Sedimentological aspects of the K/T boundary at Geulhemmerberg, Zuid Limburg, the Netherlands

Romein, A.J.T., H. Willems & H. Mai (this issue) Calcareous nannoplankton of the Geulhemmerberg K/T boundary section, Maastrichtian type area, the Netherlands

Smit, J. & R. Rocchia (this issue) Neutron activation analysis of trace elements in the Geulhemmerberg Cretaceous/Tertiary boundary section, SE Netherlands

Smit, J. & A.J.T. Romein 1985 A sequence of events across the Cretaceous-Tertiary boundary – Earth Planet. Sci. Lett. 74: 155–170

Smit, J. & W.J. Zachariasse (this issue) Planktic foraminifera in the Cretaceous/Tertiary boundary clays of the Geulhemmerberg (SE Netherlands)

Swinburne, N.H.M., A. Montanari & D.J. Depaulo (submitted) Strontium isotope stratigraphy of the Campanian-Paleocene interval based on pelagic carbonate sequences of the Umbria-Marche basin (NE Apennines, Italy) – Geochim. Cosmochim. Acta

Vonhof, H.B. & J. Smit (in prep.) A detailed Late Maastrichtian–Early Danian oceanic $^{87}Sr/^{86}Sr$ record: implications for the events around the Cretaceous-Tertiary boundary

Willems, H. (this issue) Calcareous dinocysts from the Geulhemmerberg K/T boundary section (Limburg, SE Netherlands)

Yamamoto, M., K. Ficken, M. Baas H.-J. Bosch & J.W. de Leeuw (this issue) Molecular palaeontology of the earliest Danian at Geulhemmerberg (the Netherlands)

Zijlstra, J.J.P. 1994 Sedimentology of the Late Cretaceous and Early Tertiary (tuffaceous) chalk of northwest Europe – Geol. Ultraiectina 119, 192 pp